Available online at www.sciencedirect.com
ScienceDirect
Tribology International 41 (2008) 443–448
TRIBOLOGY INTERNATIONAL
www.elsevier.com/locate/triboint

A study of the brush/rotor interface of a homopolar motor using acoustic emission

B. Raeymaekers*, D.E. Lee, F.E. Talke

Center for Magnetic Recording Research, University of California San Diego, La Jolla, CA 92093-0401, USA

Received 30 May 2007; received in revised form 28 September 2007; accepted 3 October 2007
Available online 19 November 2007

Abstract

Acoustic emission transducers were used to study the brush/rotor interface of a homopolar motor as a function of design parameters such as speed and load. The results indicate that acoustic emission is well suited for in situ monitoring of brush wear and rotor conditions, and for analyzing the tribological phenomena occurring at the brush/rotor interface.

Keywords: Acoustic emission; Homopolar motor; Brush wear

1. Introduction

Homopolar motors have been proposed as an alternative means of propulsion for ships and submarines due to their high efficiency, high power to volume ratio, and quiet operation [1–4]. In a homopolar motor, a high current is applied to a conductive rotor within a magnetic field. A net torque T is imparted on the rotor according to $T=(B\times I)r$, where B is the magnetic induction, I is the electric DC-current, and r is the radius of the rotor [5]. The current is transferred from the stator to the rotor through oxygen-free high-conductivity copper (OFHC) wire brushes which are in sliding contact with the copper rotor. Positive polarity brushes carry current from stator to rotor, while negative polarity brushes carry current in the opposite direction. It was experimentally observed that the wear rate of the positive polarity brushes is approximately one order of magnitude higher than the negative polarity brushes [6]. Since homopolar motors are required to operate for extended periods of time without maintenance, a thorough understanding of wear phenomena at the brush/rotor interface is desirable.

Only a few published papers are available concerning wear and wear-related phenomena at a copper brush/copper rotor interface. Kuhlmann Wilsdorf reported on a number of phenomena taking place at brush/rotor interfaces but did not investigate the case of a copper rotor in contact with a copper brush [7]. This paper tries to fill this gap and investigates the use of acoustic emission (AE) sensors as in situ monitoring devices to study the tribological characteristics of the brush/rotor interface in a homopolar motor. The use of AE sensors to detect contact and friction has already proven its usefulness in hard disk drive research [8,9].

2. Acoustic emission as a diagnostics tool

Acoustic emission is related to transient elastic stress waves generated during elastic and plastic deformation of materials under load. AE has been demonstrated to be useful in detecting and monitoring tribological phenomena, such as friction and wear [8–11]. The root-mean-square (RMS) of the AE signal can be expressed as

$$V_{\mathrm{RMS}}=\left[\frac{1}{\Delta t}\int_0^{\Delta t}V^2(t)\,\mathrm{d}t\right]^{1/2} \tag{1}$$

where $V(t)$ is the AE signal and Δt is the time interval over which the signal is recorded. The RMS of the AE signal is representative of the energy content of the signal [12–14]. It has been shown that the AE signal is related to the energy consumption taking place at sliding interfaces [15] and the

*Corresponding author. Tel.: +1 858 534 7578; fax: +1 858 534 2720.
E-mail address: bart@talkelab.ucsd.edu (B. Raeymaekers).

0301-679X/$ - see front matter
doi:10.1016/j.triboint.2007.10.006

overall material removal rate in manufacturing processes [16,17].

3. Sources of AE at the brush/rotor interface in a homopolar motor

Fig. 1(a) shows a close-up of a typical brush in a homopolar motor. The brush consists of a large number of copper fibers, tied together in a copper maze. AE is generated through the elastic perturbation of the brush fibers as they interact with the surface of the moving rotor, illustrated schematically in Fig. 1(b). Simulation of the fiber motion by Moon [18] has shown that the resonant frequencies of the brush fibers are in the kilohertz regime. Elastic waves generated at the brush/rotor interface propagate along the fiber into the brush housing and are finally detected by an AE sensor attached to the brush housing (see Fig. 2(b)).

4. Experimental setup

A schematic of the homopolar motor test rig and instrumentation setup is shown in Fig. 2. The test rig is designed to simulate the sliding contact between brush and rotor. In the test rig, the magnetic field is absent and the rotor is driven by a belt-transmission and an AC-motor. A copper brush is loaded with a dead weight onto a copper disc rotating at 1500 rpm (equivalent to 15 m/s surface velocity). A fiber optic probe is used to measure the vertical brush position and, thus, brush wear and wear rate. An AE sensor is mounted on the brush housing. A laser Doppler vibrometer (LDV) was used to measure brush vibrations.

A high-current power supply was used to apply both positive and negative electrical current to the brush to simulate the current density typically found in a homopolar motor (up to 160 A/cm^2).

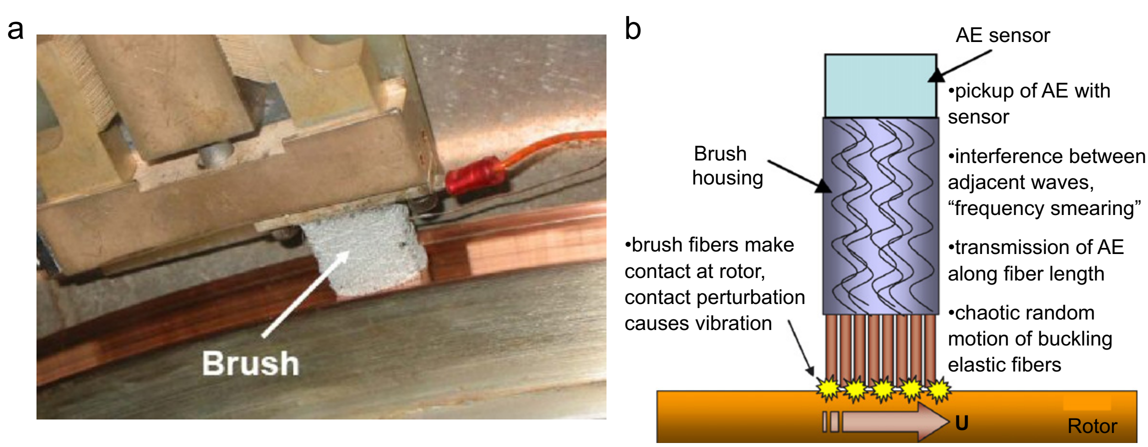

Fig. 1. (a) Close-up of the brush/rotor interface and (b) AE sources at the brush/rotor interface.

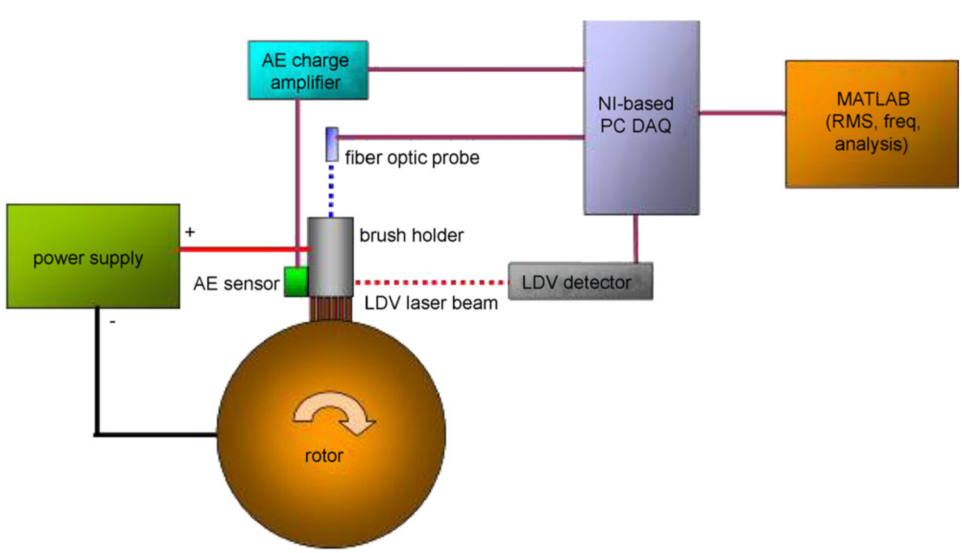

Fig. 2. Homopolar motor test rig instrumentation.

5. In situ monitoring of the homopolar motor brush/rotor interface

5.1. Type of contact

To investigate the dependence of AE on the type of contact at the brush/rotor interface, AE signals are obtained from (a) a single brush in contact with the rotor, (b) a single fiber protruding outwards by 1 mm from the brush surface, and (c) a solid copper pin with a diameter of 11 mm (7/16 in.). The power densities of all three AE signals are shown in Fig. 3.

From Fig. 3 we observe a number of differences in the frequency spectrum of the three types of contacts. In particular, the AE signal of the brush shows a nearly flat frequency response over the range from 0 to 250 kHz, similar to white noise. The single fiber exhibits also a flat frequency response, although at a signal level roughly two orders of magnitude lower than that of the brush. The solid pin, on the other hand, shows the presence of several peaks that appear to be associated with harmonics of the pin/rotor system. We postulate that the AE signal of the brush is a combination of AE events from many individual fibers, yielding a flat white noise distribution similar to that of a single fiber, but of greater amplitude.

5.2. Brush contact monitoring

Fig. 4 shows the AE signal at the brush/rotor interface for various load conditions.

We observe that an increase in the contact force (contact pressure) results in an increased AE signal. This increase in the AE signal is likely due to the increase in contact area between the brush and rotor, as a result of increased contact pressure at the interface.

Fig. 5 shows the AE RMS voltage for measurements on both a positive and negative polarity brush. The homopolar motor was continuously run at a surface velocity of 15 m/s, with current densities ranging from 0 to 160 A/cm^2, and brush pressure ranging from 0 to 140 kPa.

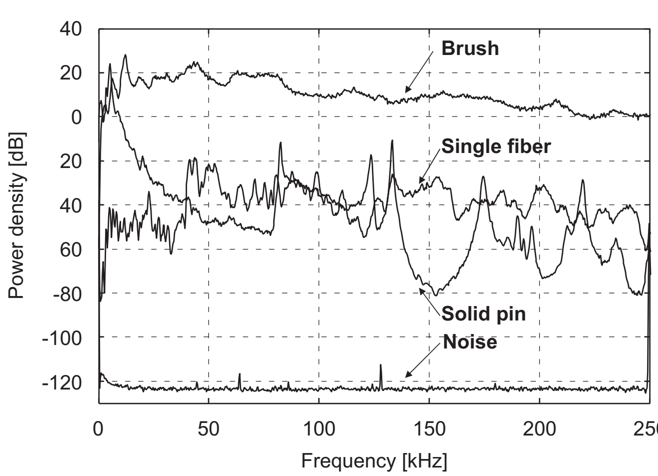

Fig. 3. Power density for different sliding contacts.

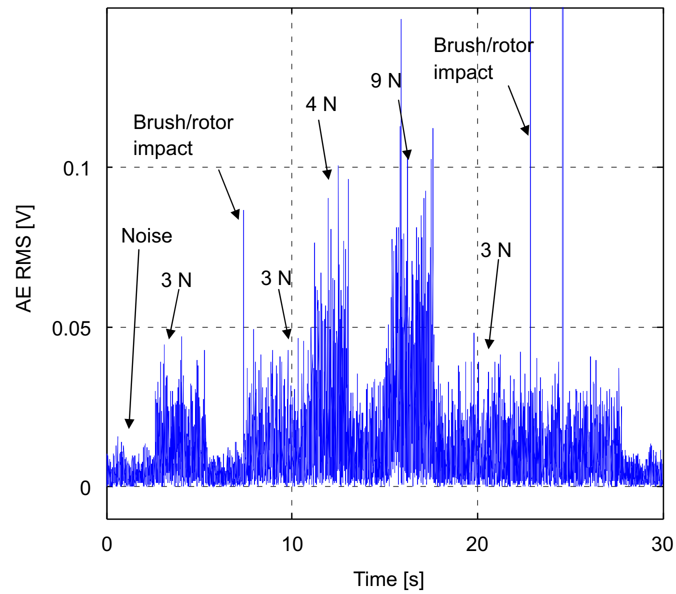

Fig. 4. Brush contact force monitoring with AE RMS voltage.

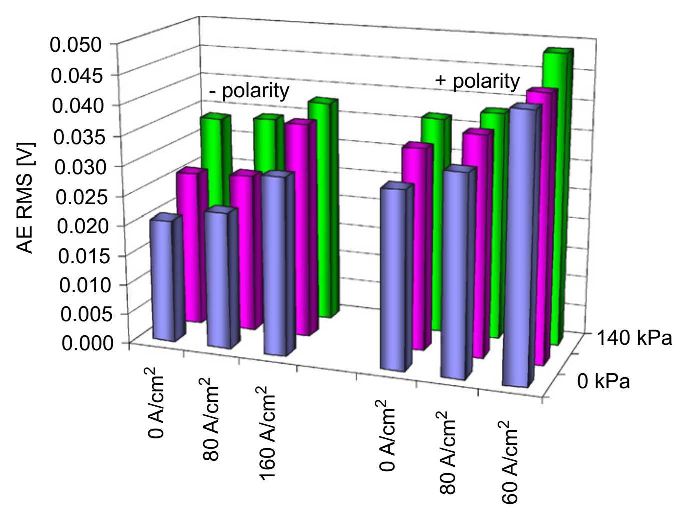

Fig. 5. AE RMS values for positive and negative polarity brush for different contact pressures and current densities.

We observe an increase in AE RMS for increasing brush pressure. This observation is in agreement with the results shown in Fig. 4 and appears to be related to the increase in contact area at the brush/rotor interface as a result of increasing contact pressure. We also observe that the AE signal increases for increasing current density.

5.3. Brush wear monitoring

Fig. 6 shows the decrease in brush length due to wear as a function of sliding distance (15 m/s surface velocity and 12 kPa contact pressure). The average non-dimensional wear rate, defined as the ratio of the wear and the sliding distance, was calculated to be $3E{-}10$.

Fig. 7 shows the RMS value of the AE signal and the wear rate as a function of the sliding distance. After an initial wear-in period, the non-dimensional wear rate is seen to approach a constant value of approximately $2E-10$. We observe that the AE signal is proportional to the wear rate.

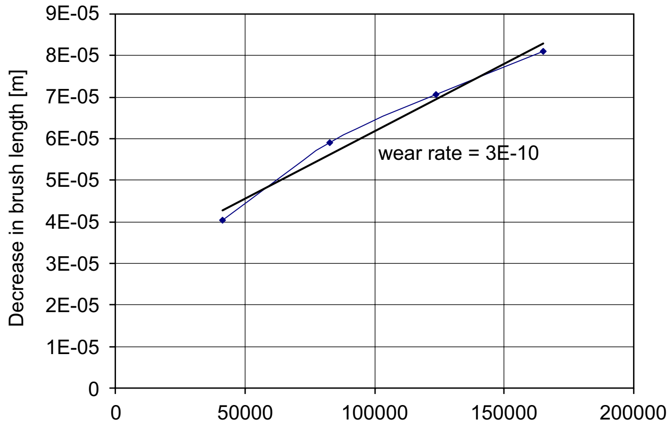

Fig. 6. Decrease in brush length versus sliding distance.

Fig. 8 shows the AE signal as a function of contact pressure and current density. A reduction in both the AE signal and the wear rate is observed for negative polarity brushes compared to positive polarity brushes.

5.4. Arcing and rotor wear

Arcing at the brush/rotor interface causes accelerated brush wear and pitting of the rotor surface. Arcing can occur due to insufficient brush preload, which might create an air gap between individual brush fibers and the rotor surface.

Fig. 9(a) shows the time frequency analysis of the AE signal. Intermittent brush/rotor contact can be observed as increased amplitude for frequencies from 0 to 800 kHz. Time frequency analysis of the AE signal during arcing is shown in Fig. 9(b). The primary difference between arcing and non-arcing is the presence of broadband white noise peaks indicated by the arrows in Fig. 9(b)).

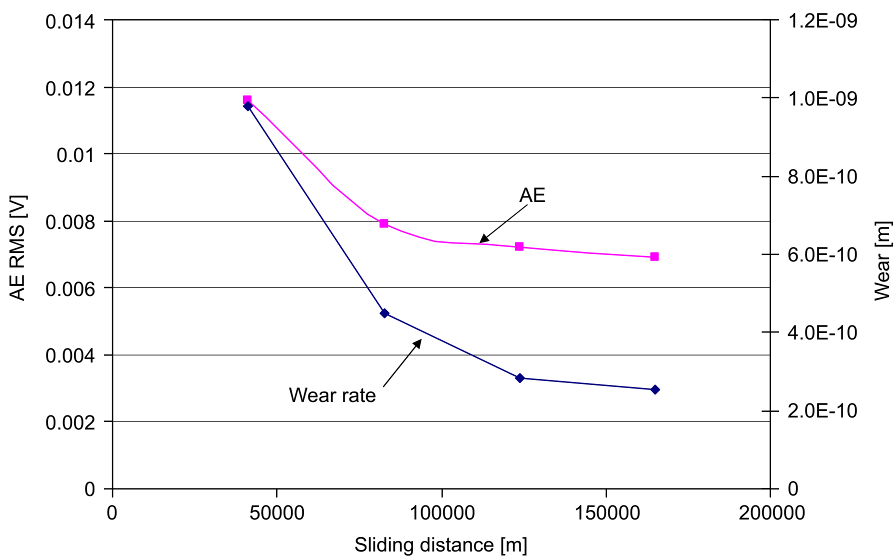

Fig. 7. Correlation of brush wear and AE.

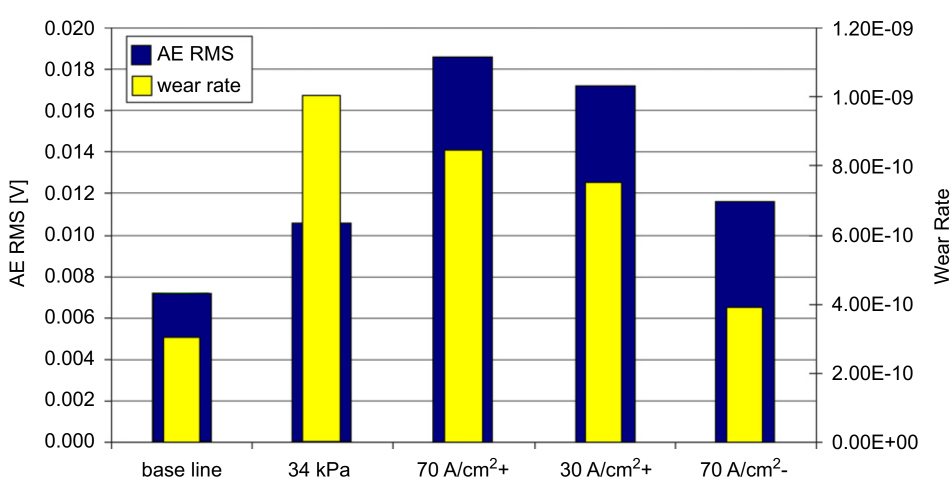

Fig. 8. AE RMS and wear rate as a function of contact pressure and current density.

Since the rotor surface directly influences overall brush wear, controlled surface finish conditions were created on the rotor surface. In Fig. 10, the time frequency analysis of the AE signal is shown for a surface with R_t roughness values of 9, 16, and 21 μm, respectively.

We observe higher frequency content in the AE signal with increasing roughness of the rotor surface.

6. Discussion

A homopolar motor operates in a sealed environment. To insure reliable operation, monitoring of the rotor and brush condition is of primary concern. AE sensors are very well suited to check the brush/rotor interface in real-time and provide feedback about possible defects and malfunctioning of the homopolar motor. Moreover, recording

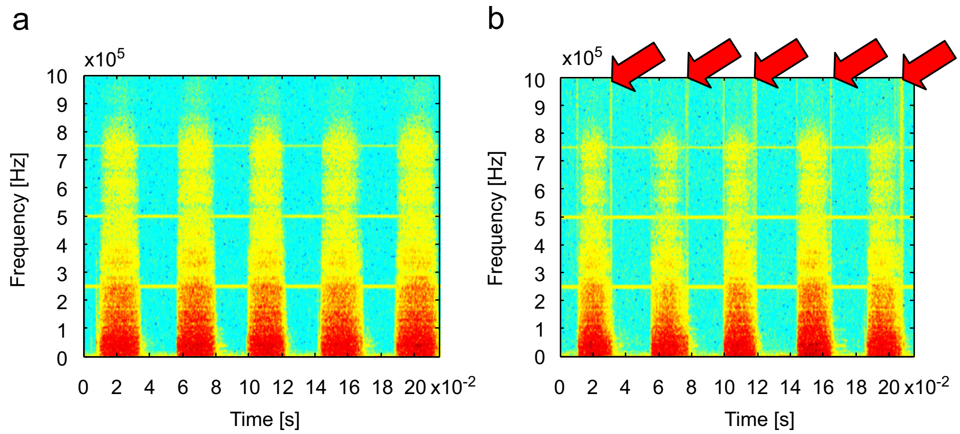

Fig. 9. Time frequency analysis of AE signal for (a) non-arcing and (b) arcing.

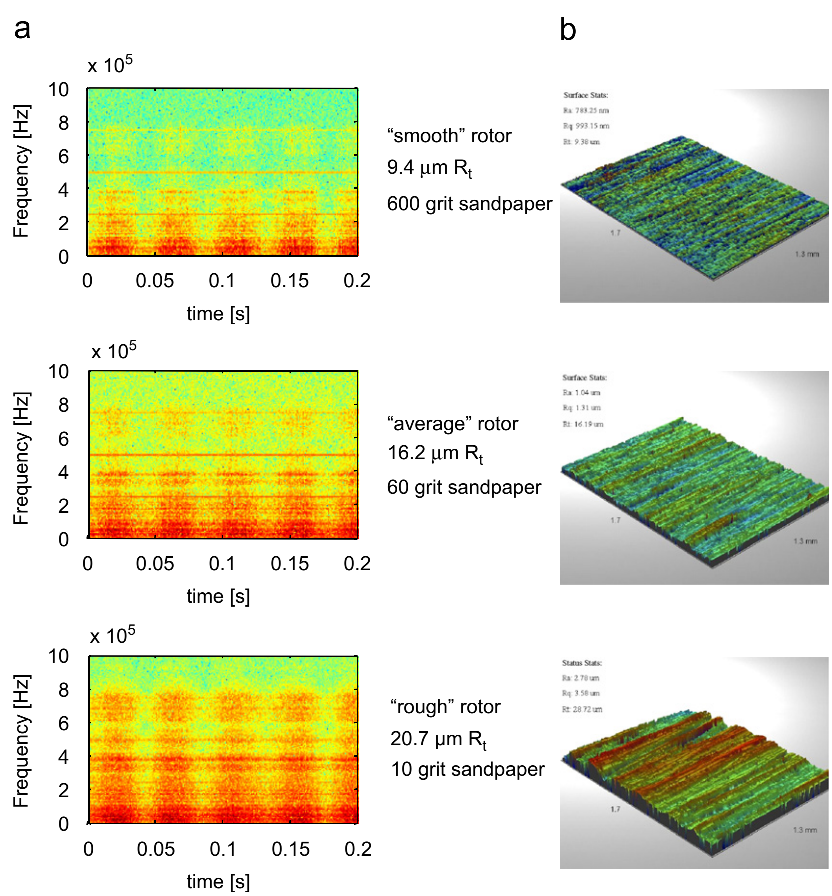

Fig. 10. Time frequency analysis of AE signal for different rotor surface conditions.

the RMS value of the AE signal enables to track the wear rate of the brush as a function of time or sliding distance. Monitoring wear and wear rate allows predicting maintenance intervals.

Current density and especially current polarity have a significant effect on brush wear, as can be seen from the results presented in this paper. To insure uniform wear of both positive and negative polarity brushes, the polarity of the brushes could be flipped for a certain period of time. AE sensors can play a crucial role in determining the "right" time to flip the brush polarity to maintain uniform brush wear, regardless of polarity.

Brush wear creates debris under the form of copper dust and copper particles among others. Wear particles may damage the rotor surface and create abrasive wear which increases the rotor surface roughness. This, in turn, will accelerate brush wear. Monitoring the frequency content of the AE signal returns information about the rotor surface condition and allows detecting excessive wear debris at an early stage.

Finally, it is interesting to point out the similarities between the research described in this paper and the experimental study of slider/disk contact in hard disk drive research [8,9]. Although the slider in a hard disk drive is a solid body, opposed to a multi-fiber brush in a homopolar motor, the experimental techniques employed are analogous and the results related to detecting contact and impact are akin.

7. Conclusion

Acoustic emission has been demonstrated to be an effective tool for in situ monitoring of a wide range of phenomena taking place in a homopolar motor. We conclude that:

1. The AE signal is sensitive to brush load, electric current density, rotor surface finish and arcing.
2. The AE signal seems to be proportional to the brush wear rate. Hence, the AE signal can be used to monitor the brush condition and its evolution in terms of wear.
3. The time frequency analysis of the AE signal yields information about the rotor condition. Higher frequency content might correlate to a rougher rotor surface.

Acknowledgments

The assistance and advice of Mr. Dariusz Appelt, Mr. Mike Condon, Dr. Z.B. Piec of General Atomics and Dr. Irwin Singer of the Naval Research Laboratory is greatly appreciated. This work was supported by the US Office of Naval Research (award # N00014-05-1-0589). We would like to acknowledge and thank Dr. S. Schreppler for his interest in this work.

References

[1] Appleton AD. Design and manufacture of a large superconducting homopolar motor (and status of superconducting ac generator). IEEE Trans Mag 1983;19(3):1047–50.
[2] Walters JD, Sondergaard NA, Levedahl J, Waltman D, Golda EM, Fikse TH. Reexamination of superconductive homopolar motors for propulsion. Nav Eng J 1998;110(1):107–16.
[3] Superczynski MJ, Waltman DJ. Homopolar motor with high temperature superconductor field windings. IEEE Trans Appl Supercond 1997;7(2):513–8.
[4] Hazelton DW, Gardner MT, Rice JA, Walker MS, Trautwein CM, Haldar P, Gubser DU, Superczynski M, Waltman D. HTS coils for the Navy's superconducting homopolar motor/generator. IEEE Trans Appl Supercond 1997;7(2):664–7.
[5] Guala-Valverde J, Mazoni P, Achilles R. The homopolar motor: a true relativistic engine. Am J Phys 2002;70(10):1052–5.
[6] Holm R. Electric contacts. Theory and application. New York/Berlin: Springer; 1967.
[7] Kuhlmann Wilsdorf D. Electrical fiber brushes—theory and observations. IEEE Trans Compon Pack Trans 1996;19(3):360–75.
[8] Knigge B, Talke FE. Contact measurement using acoustic emission analysis and system identification methods. Tribol Int 2000;33:639–46.
[9] Matsumoto M, Iida A, Hamaguchi T. Measurement of slider/disk collision forces using acoustic emission source wave analysis. Tribol Trans 1993;36(4):736–40.
[10] Sviridenok AI. Acoustic and electrical methods in triboengineering. New York: Allerton Press; 1987.
[11] Baranov V, Kudryaytsev E, Sarychev G, Schavelin V. Acoustic emission in friction. Elsevier; 2006.
[12] Clough RB. The energetics of acoustic emission source characterization. Mater Eval 1987;45:556–63.
[13] Yan T, Jones BE. Traceability of acoustic emission measurements using energy calibration methods. Meas Sci Technol 2000;11:L9–L12.
[14] Raeymaekers B, Talke FE. Characterization of tape edge contact force with acoustic emission. J Vib Acoust Trans ASME 2007;129(4):525–9.
[15] Kannatey-Asibu E, Dornfeld D. Quantitative relationships for acoustic emission from orthogonal metal cutting. J Eng Ind Trans ASME 1981;103(3):330–40.
[16] Lee DE, Hwang I, Dornfeld D. Precision manufacturing process monitoring with acoustic emission. In: Proceedings of AC'04, Zakopane, Poland, 2004.
[17] Lee DE, Hwang I, Valente CM, Oliveira JF, Dornfeld DA. Precision manufacturing process monitoring with acoustic emission. Int J Machine Tools Manuf 2006;46(2):176–88.
[18] Moon F. Chaotic vibrations. New York: Wiley; 1987.